CrystEngComm

PAPER

View Article Online
View Journal | View Issue

Cite this: *CrystEngComm*, 2015, **17**, 4325

Thermodynamic, energetic, and topological properties of crystal packing of pyrazolo[1,5-*a*]pyrimidines governed by weak electrostatic intermolecular interactions†

Clarissa P. Frizzo,*[a] Aniele Z. Tier,[a] Izabelle M. Gindri,[b] Alexandre R. Meyer,[a] Gabrielle Black,[a] Andrei L. Belladona[a] and Marcos A. P. Martins[a]

Received 27th March 2015,
Accepted 30th April 2015

DOI: 10.1039/c5ce00613a

www.rsc.org/crystengcomm

A series of pyrazolo[1,5-*a*]pyrimidines was used as a molecular model in order to understand the crystal packing of compounds with weak electrostatic intermolecular interactions. Additionally, the relationship between the energetic content of intermolecular interactions, the contact surfaces of molecules, and the thermodynamic properties of the crystal was established. The approach, which is based on a supramolecular cluster, shows that for compounds with weak electrostatic intermolecular interactions, the energetic content of the interactions is associated with a large contact surface. The crystal packing of the studied compounds is mainly governed by interactions that involve high interaction energy over a large contact surface. These results show that π···π interaction may be as responsible as other strong interactions for driving the crystal packing of compounds with weak electrostatic intermolecular interactions. Furthermore, the correlation between sublimation enthalpy and cluster energy showed that the theoretical calculation of cluster energy provided the real energetic content of crystal lattice energy and confirmed that the first coordination sphere (the supramolecular cluster) is the smallest portion of the crystal that represents all the information necessary for understanding the intermolecular interactions over the entire crystal.

Introduction

The rational development of functional molecular solids is currently the main focus of crystal engineering and it has both practical and scientific relevance in relation to understanding which parts in a molecule can provide a solid material with specific characteristics. The major challenge of crystal engineering is to establish the relationship between molecular structure and crystal packing and physical properties, to then be able to control the development of new solids with the desired physical and chemical properties. Currently, the most used tool by crystallographers is the study of the nature of inter- and intramolecular interactions in terms of directionality and distance between atoms. From this point of view, it has been proposed that crystals are constructed from supramolecular synthons, which are composed of molecules interacting through non-covalent intermolecular interactions such as hydrogen bonds, π-stacking, and halogen bonds. These interactions form robust supramolecular synthons that drive the crystallization process and the crystal packing.[1] In other words, these intermolecular interactions are molecular fragments that contain reasonable approximations of the entire crystal organization.[1–3] This theory is sometimes efficient when a specific and limited number of strong interactions is observed. The existence of such contacts is usually established on the basis of interatomic distances between interacting fragments (distance between parallel aromatic rings, hydrogen atoms, and heteroatoms). However, in the case of the presence of numerous weak electrostatic interactions, it is difficult to explain the main crystal packing pattern based only on geometric parameters of intermolecular interactions. Therefore, this strategy has proven to be limited and sometimes controversial.[4] A second approach to understanding the forces involved in directing the crystal packing was introduced by Blatov *et al.*[5] This approach assumes that the interactions between molecules are weak and non-linear, and that the arrangement of molecules to form a crystal mainly depends on the crystal packing efficiency. Hence, better organization will be achieved if the space is occupied more

[a] *NUQUIMHE, Department of Chemistry, Federal University of Santa Maria, Santa Maria, 97105-900, Brazil. E-mail: clarissa.frizzo@gmail.com*
[b] *Department of Bioengineering, University of Texas at Dallas, Richardson, Texas, 75080, USA*

† Electronic supplementary information (ESI) available. CCDC 1056486–1056491, 914143, and 734998–735002. For ESI and crystallographic data in CIF or other electronic format see DOI: 10.1039/c5ce00613a

efficiently, with reduced gaps between each molecule. Therefore, this hypothesis considers that the strength of intermolecular interactions is directly related to the contact surface between the molecules in the crystal.[5] The aforementioned tools bring approaches that take into account the thermodynamics of the crystallization process. The total lattice energy can be assessed experimentally by measuring the sublimation enthalpy[6] or by using theoretical tools, such as computational calculation.[7,8] An approach that considers the energetic aspects as well as electrostatic and contact surface complementarities is highly desirable and can promote better understanding of the relationships between molecular structure and crystal packing and physical properties. Recently, we proposed an approach for the characterization of crystallization which considers the topological and energetic properties of crystal.[9,10] According to this approach, the crystal should be analyzed as a lattice that grows from a supramolecular cluster. Considering a molecule (M_1), the cluster is formed by M_n molecules in the first coordination sphere.

In this context, the aim of this paper is to understand the crystal packing characteristics of compounds with weak electrostatic intermolecular interactions, using the supramolecular cluster approach. Additionally, we are proposing the establishment of the relationship between the topological and energetic properties of crystal and their thermodynamic and thermophysical characteristics. In order to conduct this investigation, a series of twelve pyrazolo[1,5-*a*]pyrimidines was selected, due to the crystal packing of these molecules being governed by weak electrostatic interactions. Furthermore, to evaluate this relationship, experimental measurements such as sublimation enthalpy will be used in combination with surface parameters including the topological, geometrical, and energetic data.

Results and discussion

Compounds **1–12** are fused heterocycles, better known as 2,7-disubstituted pyrazolo[1,5-*a*]pyrimidines. The numbering of the pyrazolo[1,5-*a*]pyrimidines studied in this work was established according to the variations in R^3, R^5, and R^7, as shown in Fig. 1. The compounds were grouped depending on the substituent in R^7: for compounds **1–4**, $R^7 = CCl_3$; for compounds **5–8**, $R^7 = CF_3$; and for compounds **9–12**, R^7 = aryl/heteroaryl. All the pyrazolo[1,5-*a*]pyrimidines have one methyl group bound to the C2, as well as a trihalomethyl or an aryl group bound to the C7. Pyrimidine and pyrazole rings are almost in the same plane (gap of 3.6° and they are topologically planar). The fused system is aromatic and contains ten π-electrons. An interesting characteristic of this fused π-electron system is that it contains a π-excessive ring (pyrazole) and a π-deficient ring (pyrimidine). This complementarity of pyrazole and pyrimidine rings contributes to the promotion of π···π interactions. Additionally, some compounds contain halogen atoms in their structures; therefore, crystal packing is subject to halogen interactions. Finally, it is important to note that pyrazolo[1,5-*a*]pyrimidine compounds do not possess any other polar group that would be able to participate in classical hydrogen bonds.

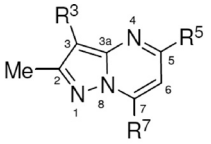

Cmp.	R^3	R^5	R^7	Cmp.	R^3	R^5	R^7
1	H	Me	CCl_3	**7**	H	C_6H_4-4-Br	CF_3
2	H	Pr	CCl_3	**8**	H	Naphth-2-yl	CF_3
3	Br	H	CCl_3	**9**	H	H	Ph
4	Br	Me	CCl_3	**10**	H	H	C_6H_4-4-F
5	H	C_6H_4-4-Me	CF_3	**11**	H	H	C_6H_4-4-Br
6	H	C_6H_4-4-Cl	CF_3	**12**	H	H	Pyrid-2-yl

Fig. 1 Structure of the pyrazolo[1,5-*a*]pyrimidines studied in this work.

Supramolecular cluster approach

In considering the supramolecular cluster approach, it is worth remembering that the supramolecular cluster of a crystal is formed by a given central molecule (M_1) that is in contact with other M_n molecules and forms the first coordination sphere. In this manner, a molecular coordination number (MCN) can be determined. The MCN has already been proposed by Kitaigorodskii[11] as being the number of molecules having at least one point of contact with a given central molecule, which is achieved by applying the principle of close-packing organic crystals.[11] The Voronoi–Dirichlet polyhedron (VDP) concept may be used to find the MCN. The VDP molecular concept was introduced by Fischer and Koch[12] in order to find the number of neighboring molecules that are in contact with a given central molecule. A Russian research group has exploited this concept and has worked systematically to determine the MCN of the first molecular coordination sphere for a large number of organic molecules.[5,13–17] In the same way, here we used VDP analyses to determine the number of neighboring molecules (MCN) in contact with the M_1, as well as the contact area between the M_1 and M_n molecules ($C_{M1\cdots Mn}$). The VDP of the central M_1 molecule was built for each of the compounds **1–12**. Fig. 2 shows the VDP[18] obtained for compound **1**, as well as the M_n molecules in contact with M_1, which form the supramolecular cluster. The first coordination sphere of the supramolecular cluster of compounds **1–12** was obtained using the VDP analyses. The MCN values were: 14 molecules for compounds **1–3**, **5**, and **8–12**; 16 molecules for compound **4**; and 18 molecules for compounds **6** and **7** (Table 2).

In accordance with the supramolecular cluster approach, the conception of crystal stability necessarily passes through the determination of the amount of energy for M_1 and each M_n molecule in the first coordination sphere of the cluster.

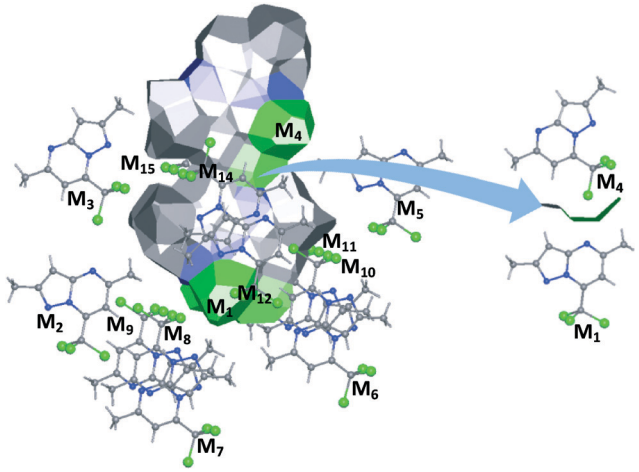

Fig. 2 (a) VDP of M_1 and supramolecular cluster for compound **1**; (b) detail of contact surface ($C_{M1\cdots M4}$) for the $M_1\cdots M_4$ of compound **1**.

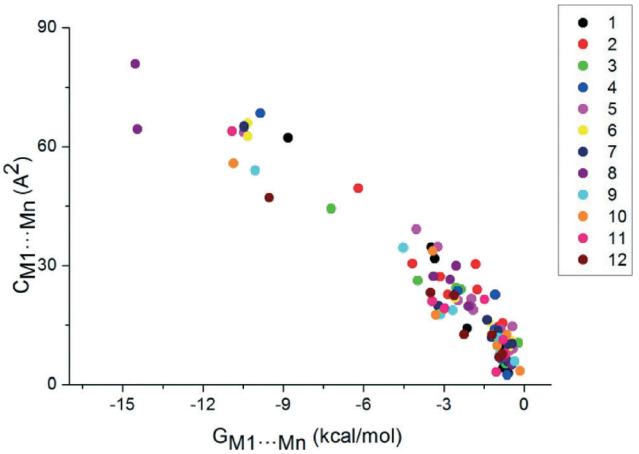

Fig. 3 Correlation between interaction energy and contact area for the molecules that are part of the cluster in the first coordination sphere of compounds **1**–**12**.

Subsequently, the intermolecular interaction energies for $M_1\cdots M_n$ dimers were calculated from the difference between double the M_1 (by itself) energy and the total energy of each of the $M_1\cdots M_n$ dimers (*i.e.*, $M_1\cdots M_2$, $M_1\cdots M_3$, …, $M_1\cdots M_n$). Thus, the energy resulting from the interaction between M_1 and each M_n molecule of the cluster ($G_{M1\cdots Mn}$) was determined for all dimers.[9] The energy of $M_1\cdots M_n$ ($G_{M1\cdots Mn}$) and the contact surface of $M_1\cdots M_n$ ($C_{M1\cdots Mn}$) were calculated for each dimer of the clusters of compounds **1**–**12** using quantum mechanical calculations. The results for compound **1** are given in Table 1, and the results for compounds **2**–**12** are given in the ESI.† From the $C_{M1\cdots Mn}$ and $G_{M1\cdots Mn}$ data (Table 1) it was possible to establish a relationship between the contact area of each M_n molecule (that is part of the first coordination sphere) and the central molecule M_1 and the interaction energy of the corresponding $M_1\cdots M_n$ dimer that is part of the cluster in the first coordination sphere. The data for compounds **1**–**12** were used and the correlation is shown in Fig. 3. The plot shows that the larger the contact surface, the larger the dimer stabilization energy (more negative energy). The correlation between $C_{M1\cdots Mn}$ and $G_{M1\cdots Mn}$ for each compound resulted in correlation coefficients ranging from 0.95 to 0.99 — the overall correlation observed for all the dimers of compounds **1**–**12** was 0.92. Therefore, it can be seen that the hypothesis proposed by Blatov *et al.*[5] was confirmed — it considers that the strength of intermolecular interactions is directly related to the contact surface between the molecules in the crystal. Considering the linear behavior of the compounds evaluated in this study, the linear equation obtained from the plot of all compounds (shown in Fig. 3) can be used to predict the energy content in dimers of other similar compounds.

Table 1 Energy and the contact surface of $M_1\cdots M_n$ ($C_{M1\cdots Mn}$) for compound **1**

Dimer	$G_{M1\cdots Mn}$ (kcal mol^{-1})[a]	$C_{M1\cdots Mn}$ (Å^2)[b]
$M_1\cdots M_2$	−0.60	10.29
$M_1\cdots M_3$	−0.84	10.69
$M_1\cdots M_4$	−2.13	14.15
$M_1\cdots M_5$	−0.60	10.29
$M_1\cdots M_6$	−2.13	14.15
$M_1\cdots M_7$	−0.84	10.69
$M_1\cdots M_8$	−0.79	4.16
$M_1\cdots M_9$	−0.74	8.63
$M_1\cdots M_{10}$	−3.34	31.76
$M_1\cdots M_{11}$	−3.48	34.65
$M_1\cdots M_{12}$	−0.59	2.76
$M_1\cdots M_{13}$	−0.61	2.76
$M_1\cdots M_{14}$	−8.82	62.25
$M_1\cdots M_{15}$	−8.82	62.25

[a] Determined using the equation $G_{M_1\cdots M_n} = (2{\cdot}E_{M_1} - E_{M_1\cdots M_n})$.[9] [b] Determined using TOPOS®.[18]

The total energy ($G_{cluster}$) and contact surface ($C_{cluster}$) of the supramolecular cluster is obtained from the sum of the energies and the sum of the contact surfaces of all dimers, respectively.[9]

The $G_{cluster}/C_{cluster}$ ratio provides the average stabilization energy distributed over the molecule in a homogeneous manner, which shows how the M_1 molecule would appear if it had its interaction energy homogeneously distributed over its surface. The $G_{cluster}/C_{cluster}$ values for compounds **1**–**12** are given in Table 2 and they range from −0.10 to −0.16 kcal mol^{-1} Å^{-2}. Similar $G_{cluster}/C_{cluster}$ values were found for compounds **1**–**7** which contain trihalomethyl groups at the 7-position of the pyrazolo[1,5-*a*]pyrimidines, as well as hydrogen, alkyl, or aryl substituents at the 5-position of the fused ring. Higher values were found for compounds **9**–**12** which have aryl groups at the 7-position and no substituents at the 5-position of the pyrazolo[1,5-*a*]pyrimidine. It was observed that compounds **1**–**4** have little $G_{cluster}$ stabilization energies and small $C_{cluster}$ values, while for compounds **5**–**8** the $G_{cluster}$ stabilization energies and $C_{cluster}$ values increase. The balance between these two parameters in both groups resulted in similar $G_{cluster}/C_{cluster}$ values. Different behaviors were verified for compounds **9**–**12**, in which $G_{cluster}$ stabilization energy increases and the $C_{cluster}$ value decreases, leading to higher $G_{cluster}/C_{cluster}$ values. Compound **8** is structurally similar to compounds **1**–**7**, but its $G_{cluster}/C_{cluster}$ value is similar

Table 2 The MCN,[a] cluster energy ($G_{cluster}$),[b] and cluster contact surface ($C_{cluster}$)[c] for the supramolecular clusters

Comp.	MCN	$G_{cluster}$ (kcal mol^{-1})	$C_{cluster}$ (Å^2)	$G_{cluster}/C_{cluster}$ (kcal mol^{-1} Å^{-2})
1	14	−34.32	279.48	−0.12
2	14	−33.51	337.30	−0.10
3	14	−34.88	288.08	−0.12
4	16	−35.08	314.48	−0.11
5	14	−40.26	350.75	−0.11
6	18	−40.34	347.00	−0.12
7	18	−43.16	350.41	−0.12
8	14	−53.12	378.54	−0.14
9	14	−41.86	282.37	−0.15
10	14	−42.60	283.50	−0.15
11	14	−42.76	295.24	−0.14
12	14	−41.72	264.38	−0.16

[a] The molecular coordination number (MCN) is the number of molecules in the supramolecular cluster formed by the first molecular coordination sphere. [b] Determined using the equation $G_{cluster} = \sum_n \left(G_{M_1\cdots M_n}\right)$.[9] [c] Determined using the equation $C_{cluster} = \sum_n \left(C_{M_1\cdots M_n}\right)$.[9]

Table 3 The normalized interaction energy ($N_{GM1\cdots Mn}$), the normalized contact surface ($N_{CM1\cdots Mn}$), and the interaction type for the supramolecular cluster of compound **1**

Dimer	N_G[a]	N_C[b]	Interaction type
$M_1\cdots M_2$	0.24	0.52	III
$M_1\cdots M_3$	0.34	0.54	III
$M_1\cdots M_4$	0.87	0.71	III
$M_1\cdots M_5$	0.24	0.52	III
$M_1\cdots M_6$	0.87	0.71	III
$M_1\cdots M_7$	0.34	0.54	III
$M_1\cdots M_8$	0.32	0.21	III
$M_1\cdots M_9$	0.30	0.43	III
$M_1\cdots M_{10}$	1.36	1.59	III
$M_1\cdots M_{11}$	1.42	1.74	III
$M_1\cdots M_{12}$	0.24	0.14	III
$M_1\cdots M_{13}$	0.25	0.14	III
$M_1\cdots M_{14}$	3.60	3.12	II
$M_1\cdots M_{15}$	3.60	3.12	II

[a] Determined using the equation $N_{G_{M_1\cdots M_n}} = \mathrm{MCN} \times \frac{G_{M_1\cdots M_n}}{G_{cluster}}$. [b] Determined using the equation $N_{C_{M_1\cdots M_n}} = \mathrm{MCN} \times \frac{C_{M_1\cdots M_n}}{C_{cluster}}$.

to compounds **9–12**. The $G_{cluster}$ and $C_{cluster}$ values for compound **8** are the highest in comparison with the other compounds; however, the $G_{cluster}$ increment was more expressive than for the $C_{cluster}$. The high increment in the energy value of compound **8** is probably due to the presence of the naphth-2-yl group at the 5-position of the fused ring. The naphth-2-yl group introduces a π⋯π interaction with 14.5 kcal mol^{-1} (dimer $M_1\cdots M_{14}$ and $M_1\cdots M_{15}$), which is about twice the energy of the same dimers in the other compounds with a π⋯π interaction.

In order to ascertain the energetic contribution of each dimer for cluster stabilization, the normalized energy ($N_{GM1\cdots Mn}$) and the normalized contact surface ($N_{CM1\cdots Mn}$) have to be determined.[9] The strength of the interaction between M_1 and any M_n molecule can be estimated based on the $N_{GM1\cdots Mn}$ and $N_{CM1\cdots Mn}$ parameters. From the $N_{GM1\cdots Mn}$ and $N_{CM1\cdots Mn}$ parameters, the intermolecular interactions were divided into four types:[9] (I) represents a molecular dimer with high interaction energy on a small contact surface (*e.g.*, hydrogen bonds); (II) involves high interaction energy on a large contact surface (*e.g.*, π⋯π interactions); (III) involves little interaction energy and contact surfaces with a maximum difference of ±0.5 between the two parameters; and (IV) is a contribution based on contact surfaces with little interaction energy. From this point of view, compounds **1–12** were analyzed. The $N_{GM1\cdots Mn}$ and $N_{CM1\cdots Mn}$ parameters for each dimer of compound **1** are shown in Table 3. The same data for compounds **2–12** are given in the ESI.†

The type II interaction has the highest stabilization energy in the supramolecular cluster for these compounds. These interactions represent dimers that have direct contact with molecules above and below the M_1 plane (Fig. 4a). These results, combined with the contact surface data, suggest that crystallization is driven by the type II interaction, and they also demonstrate the importance of π-stacking interactions in the crystal packing of pyrazolo[1,5-*a*]pyrimidines. Furthermore, it can be assumed that the π⋯π interactions may be as responsible as other interactions for driving the crystal packing of compounds with weak electrostatic intermolecular interactions. In other words, in terms of energy, π⋯π interactions can be as strong as hydrogen bonds. Type III interactions are predominant in the crystal packing of compounds **1–12** but are less important because they mainly occur due to the complementarity of surfaces (Fig. 4b and c).

Sublimation enthalpy (ΔH_{sub}) is a thermochemical quantity that represents a macroscopic measure of the magnitude of intermolecular interaction energy in a solid and, therefore, the stability of the crystal structure. In other words, it represents the energy required to break up the solid state and convert the system into the gaseous phase. Thus, from experimental determination, it is possible to quantify the energy contained in the intermolecular interactions in the crystal structure, which is essential for a suitable characterization of crystalline materials.[19] The main goal of determining sublimation enthalpy is to correlate this value with the energetic content of the supramolecular cluster and show that the microrepresentation of molecular crystal (supramolecular cluster) reflects the macro properties (*i.e.*, sublimation enthalpy). Experimentally, ΔH_{sub} can be obtained from the sum of vaporization enthalpy ΔH_{vap}(298 K) and fusion enthalpy ΔH_{fus}(298 K) (eqn (1)).

$$\Delta H_{sub}(298\ \mathrm{K}) = \Delta H_{vap}(298\ \mathrm{K}) + \Delta H_{fus}(298\ \mathrm{K}) \quad (1)$$

In this work, gas chromatography was used to measure the vaporization enthalpy (ΔH_{vap}(298 K)) in accordance with the method that was proposed by Peacock and Fuchs[20–25]

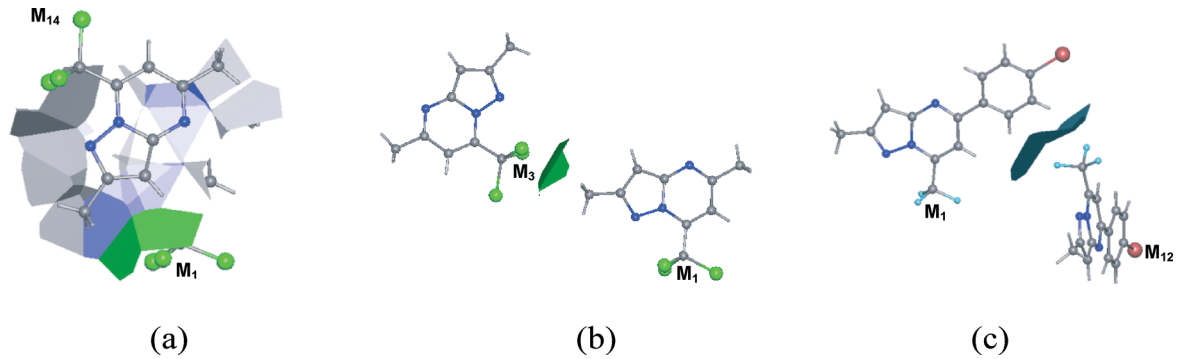

Fig. 4 (a) Type II interactions in dimer $M_1\cdots M_{14}$ (**1**); (b) type III interactions in dimer $M_1\cdots M_3$ (**1**); and (c) type IV interactions in dimer $M_1\cdots M_{12}$ (**7**).

and modified by Chickos *et al.*[26–28] The pyrazolo[1,5-*a*]-pyrimidines **1**, **5**, **6**, **7**, **9**, **12**, and **13** were chosen for this study and there were at least two compounds in each of the groups formed according to the substituent in R^7: compounds **1** and **13** with $R^7 = CCl_3$; compounds **5**, **6**, and **7** with $R^7 = CF_3$; and compounds **9** and **12** with R^7 = aryl/heteroaryl. The experimental fusion enthalpy was determined by differential scanning calorimetry (DSC) and the results were adjusted as a function of temperature at 298 K (ΔH_{fus}(298 K)), according to the protocol developed by Chickos *et al.*[26–28] The results of ΔH_{fus}(298 K), ΔH_{vap}(298 K), and ΔH_{sub}(298 K) for pyrazolo[1,5-*a*]pyrimidines are shown in Table 4.

Considering that sublimation enthalpy represents the energy of crystal lattice, it is reasonable to expect a good correlation with the $G_{cluster}$ energy. In 1999, Osborn and York[29] used force fields to find a correlation between sublimation enthalpy and lattice energy, and they determined that the Gavezzotti force field presents a better level of agreement. The authors were interested in predicting polymorphism and did not provide the correlation coefficient and linear equation resulting from the correlation.

In this study, the cluster energy (determined using quantum mechanical calculations) gave a good correlation (r = 0.91) with sublimation enthalpy (Fig. 5). These results indicate that the $G_{cluster}$ determined using quantum mechanical calculations provides a good estimation of the real energetic content. The angular coefficient of the linear equation is negative because the sublimation enthalpy has positive energy values (it is an endothermic process) and the cluster energy has a negative value (it represents the difference in the molecule's energetic content in the cluster in relation to the isolated molecule). Thus, the inversely proportional relationship is expected because the more negative the values of the stabilization energy ($G_{Cluster}$), the more positive the sublimation enthalpy values, so that the energy in the crystal lattice is correctly represented by the amount of sublimation enthalpy. The high correlation coefficients found for compounds **1**, **5**, **6**, **7**, **9**, **12**, and **13** confirm the hypothesis that the first coordination sphere is the smallest portion of the crystal that presents all the necessary information (energetic content and contact surfaces) for understanding the intermolecular interactions of the entire crystal system. It is necessary to cite here the important work performed by Perlovich *et al.*[30–35] in which the determination of sublimation thermodynamics and its correlation with certain crystal properties, such as van der Waals volume (V^{vdW}) and calculated density (D_{calc}), was performed. The authors state that in order to reveal the effect of molecular topology on crystal package architecture and thermodynamic characteristics, it is necessary to analyze the D_{calc}. Moreover, the authors argue that D_{calc} is an entropic

Table 4 The thermodynamic and thermophysical data for compounds **1**, **5**–**7**, **9**, **12**, and **13**

Comp.	ΔH_{fus}(298 K) (kcal mol^{-1})[a]	ΔH_{vap}(298 K) (kcal mol^{-1})[b]	ΔH_{sub}(298 K) (kcal mol^{-1})[c]	ΔS_{sub}(298 K) (kcal mol^{-1})
1	3.71	23.23	26.94	0.09
5	5.22	26.68	31.89	0.11
6	5.58	27.16	32.75	0.11
7	5.42	28.09	33.51	0.11
9	4.36	25.33	29.69	0.10
12	3.98	25.39	29.38	0.10
13[d]	1.94	21.77	23.70	0.08

[a] Determined from DSC and adjusted according to the protocol developed by Chickos *et al.*[26–28] [b] Determined using correlation gas chromatography. [c] Determined using eqn (1). [d] Compound **13** was included only here, because other data for it (excluding fusion enthalpy) has already been published.[9]

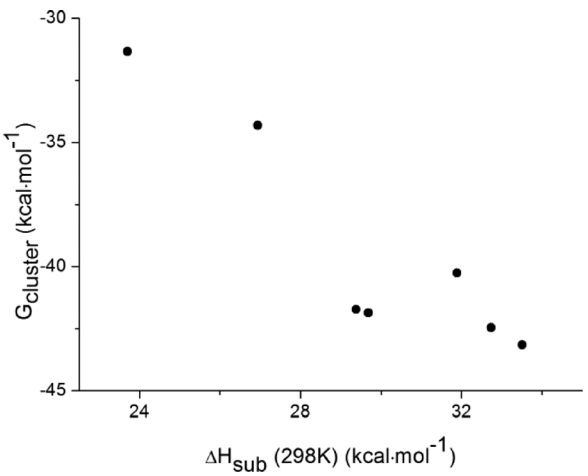

Fig. 5 Correlation between sublimation enthalpy and $G_{cluster}$ for compounds **1**, **5**, **6**, **7**, **9**, **12**, and **13**.

characteristic of a crystal, thus it should be correlated with the sublimation entropy terms. They established correlations between crystal lattice energy (Gavezzotti's field[36]) and the ratio of the free volume per molecule (V^{free}) and V^{vdW} (V^{free}/V^{vdW}), and fusion enthalpy and the melting point of organic compounds. The V^{free} was better investigated by Perlovich *et al.*[30–35] because the authors believed that this parameter may be involved in the sublimation mechanism of molecular crystals, and they considered the V^{free}/V^{vdW} ratio to be the molecular packing density. Perlovich *et al.*[30–35] obtained more success for some correlations and less success for others. Therefore, in this paper, we propose other correlations to assist the understanding of crystal packing, by exploring the interrelations between thermodynamic (sublimation) and thermophysical (fusion) characteristics, and crystal architecture parameters. For this, we focus on the existence of "voids" in the molecular crystals. "Voids" refer to the existence of void spaces between the molecules. From this, the "packing coefficient" can be defined as the ratio of molecular volume to cell volume.[37] Turner *et al.*[38] proposed a simple approach for mapping void space, using the procrystal isosurface in the Crystal Explorer software.[39] They showed how to obtain the cell volume (V_c) and void volume (V_v). Through use of these data we proposed the determination of crystal packing efficiency (CPE), using eqn (2).

$$\mathrm{CPE} = \frac{V_c - V_v}{V_c} \quad (2)$$

The CPE represents an estimation of molecules that are occupying the unity cell, as well as giving an idea of how close the molecules are in the unity cell — the closer they are, the more efficient the packing. The CPE values determined for compounds **1–12** ranged between 0.87 and 0.93. Compounds **1–8** had very similar CPE values, ranging between 0.87 and 0.89, while the values for compounds **9–12** were between 0.92 and 0.93. Considering that more efficient crystal packing will result in more energy per contact surface, it is reasonable to expect a relationship between the CPE and the $G_{cluster}/C_{cluster}$ value. When these two parameters were plotted, the correlation expected for the twelve pyrazolo[1,5-*a*]pyrimidines studied could be seen (Fig. 6a). Another geometric parameter that may be related to the CPE is the surface area per unit volume. This measurement is an important factor for molecular approximation in a crystallization process. Compounds with a large surface to volume ratio are much more likely to have good packing. Considering the importance of topological parameters driving the crystal packing, molecules will be forced to increase their contact areas in order to reduce voids between other molecules. The plot for this correlation is shown in Fig. 6b. For compounds **1–13**, there is a good correlation coefficient of $R = 0.91$ for the correlation between the CPE and the surface to volume ratio. This correlation is evidence that topology (contact surface) is an important factor driving the crystal growth of organic compounds, in which strong electrostatic interactions are absent. Other relationships for the topological properties and thermodynamic characteristics of crystal were investigated (*e.g.*, sublimation entropy terms *versus* CPE and void volume), but no correlations were detected. However, when we look at some structural aspects of the compounds, some interesting relationships can be observed after plotting the sublimation entropy terms *versus* CPE. The substitution of an H with an Me group at the 5-position of the fused ring results in a decrease in CPE and an increase in the sublimation entropy terms. Similar behavior was observed when the chlorine atom was substituted with a bromine in the aryl group attached at the 5-position of the fused ring, and when pyridin-2-yl was substituted with phenyl. However, it is difficult to attribute the increase in entropy solely to the increase in CPE. Additionally, the molecular mass effect may also be associated with these relationships. The correlation between D_{calc} and the sublimation entropy terms for some compounds

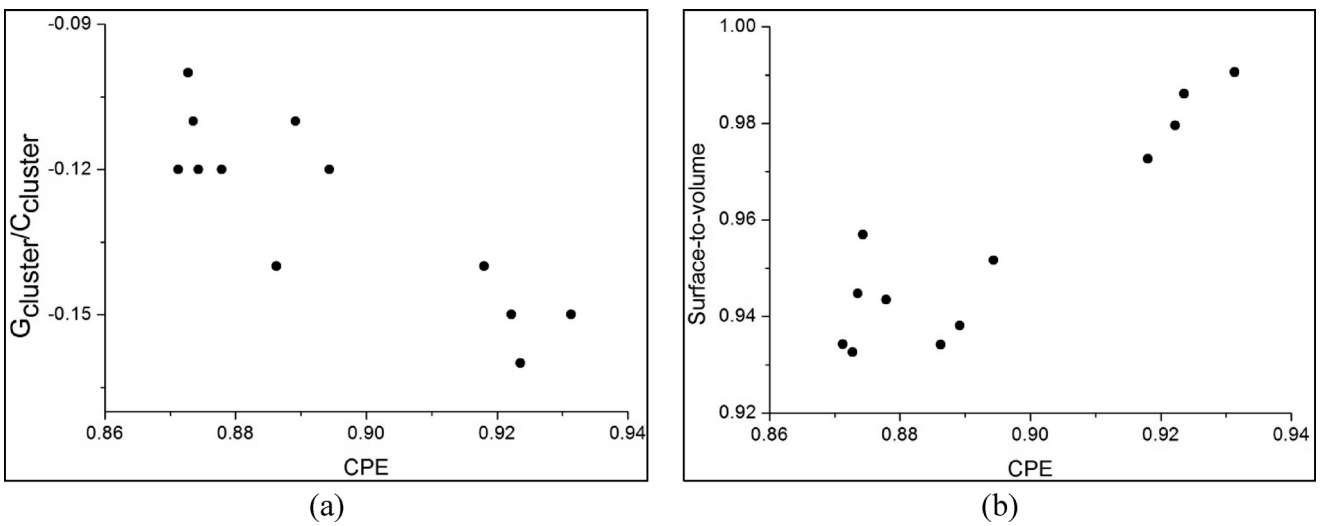

Fig. 6 (a) Correlation between the $G_{cluster}/C_{cluster}$ and the CPE for compounds **1–12**; (b) correlation between the CPE and the surface-to-volume ratio for compounds **1–12**.

was determined by Perlovich *et al.*[30–35] However, the pyrazolopyrimidines investigated here did not display this correlation. This result is reasonable, because D_{calc} takes into account the molecular weight and its variations and does not represent the properties of crystal packing. Furthermore, a correlation between D_{calc} and CPE was not found, thus confirming that these measurements represent different properties of crystal packing and are not correlated. The relationships of the packing features and molecular structure, as well as the strength and the nature of intermolecular interactions with melting point, were determined and, in general, a correlation was observed. These relationships were determined by considering that the variation in the melting points between organic molecules with very similar structures (and molecular weight) is due to the different crystal packings of molecules.[40–47] Recently, the Hirshfeld surface has been used to extend this correlation, because it is considered to be a quantitative measurement of intermolecular interactions and correlates these data with melting points.[48,49]

Conclusions

In summary, the results show that for compounds with weak electrostatic intermolecular interactions, the energetic content of the interactions is associated with the contact surface. The crystal packing of the studied compounds is mainly governed by interactions involving high interaction energy over a large contact surface. These results show that π···π interaction can drive the crystal packing of compounds with weak electrostatic intermolecular interactions. The energy of this interaction showed that it is as strong as hydrogen bonds. This interaction has been shown to be essential to stabilize and drive the crystal packing of organic molecules[50] as well as more complex systems such as polymers[51] and proteins.[52] The supramolecular approach also led to the observation that crystallization can be governed by the complementarity of surfaces. Thus, the results described here corroborate with the hypothesis that the contact surface between the molecules leads to the approximation of molecules during crystallization and it may be the driving force for the crystalline arrangement of pyrazolo[1,5-*a*]pyrimidines. Furthermore, the correlation between sublimation enthalpy and cluster energy revealed that the theoretical calculation of cluster energy provides a real estimation of the energetic content of crystal lattice energy and confirmed that the first coordination sphere (supramolecular cluster) is the smallest portion of the crystal that represents all necessary information for understanding the intermolecular interactions in the entire crystal. This hypothesis was suggested in our recent work[9] and has been used and improved in this paper.

Experimental

Synthesis

The synthesis and the complete ^{1}H and ^{13}C NMR data, mass spectrometric data, and elemental analysis of compounds **1–13** are available in the literature.[53,54] The crystals of **7** and **9** were obtained by solubilization in 5 mL of a mixture of ethanol and dimethyl sulfoxide, at a ratio of 6 : 4, followed by slow evaporation at 25 °C.

X-ray diffraction data

The diffraction measurements were done using graphite monochromatized Mo Kα radiation with λ = 0.71073 Å, on a Bruker SMART CCD diffractometer.[55] The structures were solved with direct methods using the SHELXS program, and refined on F^2 by full-matrix least-squares with the SHELXL package.[56] Absorption correction was performed using the Gaussian method.[57] Anisotropic displacement parameters for non-hydrogen atoms were applied. The hydrogen atoms were placed at calculated positions with 0.96 (methyl CH_3), 0.97 (methylene CH_2), 0.98 (methyne CH), 0.93 (aromatic CH), and 0.82 Å (OH), using a riding model. Hydrogen isotropic thermal parameters were kept equal to $U_{iso}(H) = xU_{eq.}$ (carrier C atom), with x = 1.5 for methyl groups and x = 1.2 for all others. The valence angles C–C–H and H–C–H of the methyl groups were set to 109.5°, and H atoms were allowed to rotate around the C–C bond.

Computational calculations

The intermolecular interaction energies in the supramolecular clusters of compounds **1–13** were determined by single point calculations (without optimization of molecular geometry) performed with geometries obtained from X-ray diffraction. All quantum mechanical calculations were performed with the aid of the Gaussian© 09 software package.[58] To obtain the interaction energy between each $M_1\cdots M_n$ dimer, the second-order Moller–Plesset (MP2) perturbation theory was used with a level of theory of MP2/cc-PVDZ. The counterpoise method of Boys and Bernardi[59] was employed to minimize the basis set superposition error (BSSE).

Voronoi–Dirichlet polyhedron (VDP)

The molecular Voronoi–Dirichlet polyhedron (VDP) concept was introduced in order to find the number of neighboring molecules that have contact with a given central molecule. This introduced the idea that the face of the molecular VDP is a set of atomic VDP faces corresponding to the adjacent contacts between the atoms of two molecules. From this it was established that the area of the face of a VDP corresponds to a molecular $M_1\cdots M_n$, and its contact area is determined by the strength of molecular interactions. This concept was proposed by Blatov *et al.*[13–18]

Differential scanning calorimetry (DSC)

The DSC experiments were performed using a MDSC Q2000 (T-zeroTM DSC technology, TA Instruments Inc., USA). Dry, high purity (99.999%) nitrogen gas was used as the purge gas (50 mL min^{-1}). The heating rate used for all the samples was 10 °C min^{-1}. Samples were crimped in hermetic aluminum

pans with lids. The sample mass was weighed on a Sartorius M 500 P to an accuracy of ± 0.001 mg.

Gas chromatographic studies

All compounds used in the study were obtained from Aldrich Chemical Co. and used as purchased. CGC experiments were performed on a HP 5890 Gas Chromatograph equipped with a flame ionization detector and run at a split ratio of approximately 100/1. Retention times were recorded on a HP Chemstation. The compounds were run isothermally, either on a J&W 0.25 mm, 30 m DB5MS column, or a Restek 0.5 mm, 30 m RTX-5 column. While transfer enthalpies do depend on the nature of the column used, the results following the correlation remain independent of the nature of the column within the reproducibility of the results. Column temperatures were controlled by the gas chromatograph and were monitored independently by using a Fluke digital thermometer. The temperature of the gas chromatograph was kept constant, to an accuracy of 0.1 K. Helium was used as the carrier gas.

Acknowledgements

The authors are grateful for the financial support of the National Council for Scientific and Technological Development (CNPq) – Universal/Proc. 474895/2013-0 and Universal/Proc. 475556/2012-7, the Foundation for Research Support of the State of Rio Grande do Sul (FAPERGS), and the Coordination for Improvement of Higher Education Personnel (CAPES/PROEX). The fellowships from CNPq (M. A. P. M. and I. M. G) and CAPES (A. Z. T. and A. R. M.) are also acknowledged.

References

1 G. Desiraju, *Angew. Chem., Int. Ed.*, 2007, **46**, 8342.
2 E. Nahua, E. Kolehmainen and M. Nissinen, *CrystEngComm*, 2011, **13**, 6531.
3 B. Chattopadhyay, S. Ghosh, S. Mondal, M. Mukherjee and A. K. Mukherjee, *CrystEngComm*, 2012, **14**, 837.
4 D. Chopra, V. Thiruvenkatam, S. G. Manjunath and T. N. G. Row, *Cryst. Growth Des.*, 2007, **7**, 868.
5 V. A. Blatov, *Crystallogr. Rev.*, 2004, **10**, 249.
6 J. S. Chickos and W. E. Acree, *J. Phys. Chem.*, 2002, **31**, 537–698.
7 C. Ouvrard and J. B. O. Mitchell, *Acta Crystallogr., Sect. B: Struct. Sci.*, 2003, **59**, 676–685.
8 J. G. Brandenburg, M. Alessio, B. Civalleri, M. F. Peintinger, T. Bredow and S. Grimme, *J. Phys. Chem. A*, 2013, **117**, 9282–9292 and references therein.
9 M. A. P. Martins, C. P. Frizzo, A. C. L. Martins, A. Z. Tier, I. M. Gindri, A. R. Meyer, H. G. Bonacorso and N. Zanatta, *RSC Adv.*, 2014, **4**, 44337.
10 C. P. Frizzo, C. Bender, A. Tier, P. R. S. Salbego, A. R. Meyer, M. A. P. Martins and I. M. Gindri, *CrystEngComm*, 2015, **17**, 2996–3004.
11 A. I. Kitaigorodskii, *Molecular Crystals and Molecules*, Academic Press, New York, 1973.
12 W. Fischer and E. Koch, *Z. Kristallogr.*, 1979, **150**, 245–260.
13 T. G. Mitina and V. A. Blatov, *Cryst. Growth Des.*, 2013, **13**, 1655–1664.
14 E. V. Peresypkina and V. A. Blatov, *Acta Crystallogr., Sect. B: Struct. Sci.*, 2000, **56**, 501–511.
15 E. V. Peresypkina and V. A. Blatov, *Acta Crystallogr., Sect. B: Struct. Sci.*, 2000, **56**, 1035–1045.
16 E. V. Peresypkina and V. A. Blatov, *J. Mol. Struct.: THEOCHEM*, 1999, **498**, 225–236.
17 V. A. Blatov, L. V. Pogildyakova and V. N. Serezhkin, *Z. Kristallogr.*, 1998, **213**, 202–209.
18 V. A. Blatov and A. P. Shevchenko, *TOPOS® version 4.0 software*, Samara State University, Ac. Pavlov St., 443011 Samara, Russia, http://www.topos.ssu.samara.ru.
19 A. Gavezzotti, *J. Phys. Chem.*, 1991, **95**(22), 8948–8955.
20 L. A. Peacock and R. Fuchs, *J. Am. Chem. Soc.*, 1977, 5524.
21 R. Fuchs and L. A. Peacock, *Can. J. Chem.*, 1978, **56**, 2493.
22 R. Fuchs and L. A. Peacock, *Can. J. Chem.*, 1979, **57**, 2302.
23 R. Fuchs and L. A. Peacock, *Can. J. Chem.*, 1980, **58**, 2796.
24 R. Fuchs and W. K. Stephenson, *Can. J. Chem.*, 1985, **63**, 349.
25 R. Fuchs, E. J. Chambers and W. K. Stephenson, *Can. J. Chem.*, 1987, **65**, 2624.
26 J. S. Chickos, S. Hosseini and D. G. Hesse, *Thermochim. Acta*, 1995, **249**, 41–62.
27 J. S. Chickos, S. Hosseini and D. G. Hesse, *Thermochim. Acta*, 1998, **313**, 19–26.
28 J. S. Chickos, S. Hosseini and D. G. Hesse, *Thermochim. Acta*, 1998, **313**, 101–110.
29 J. C. Osborn and P. York, *J. Mol. Struct.*, 1999, **474**, 43–47.
30 G. L. Perlovich, A. M. Ryzhakov, V. V. Tkachev, L. Kr Hansen and O. A. Raevsky, *Cryst. Growth Des.*, 2013, **13**, 4002–4016.
31 A. O. Surov, K. A. Solanko, A. D. Bond, A. Bauer-Brandl and G. L. Perlovich, *CrystEngComm*, 2013, **15**, 6054–6061.
32 A. N. Manin, A. P. Voronin, N. G. Manin, M. V. Vener, A. V. Shishkina, A. S. Lermontov and G. L. Perlovich, *J. Phys. Chem. B*, 2014, **118**, 6803–6814.
33 A. N. Manin, A. P. Voronin and G. L. Perlovich, *Thermochim. Acta*, 2014, **583**, 72–77.
34 G. L. Perlovich, A. M. Ryzhakov, V. V. Tkachev and A. N. Proshin, *CrystEngComm*, 2015, **17**, 753–763.
35 A. O. Surov, A. A. Simagina, N. G. Manin, L. G. Kuzmina, A. V. Churakov and G. L. Perlovich, *Cryst. Growth Des.*, 2015, **15**, 228–238.
36 A. Gavezzotti and G. Filippini, *J. Am. Chem. Soc.*, 1995, **117**, 12299–12305.
37 C. J. Eckhardt and A. Gavezzotti, *J. Phys. Chem. B*, 2007, **111**, 3430–3437.
38 M. J. Turner, J. J. McKinnon, D. Jayatilaka and M. A. Spackman, *CrystEngComm*, 2011, **13**, 1804–1813.
39 S. K. Wolff, D. J. Grimwood, J. J. McKinnon, M. J. Turner, D. Jayatilaka and M. A. Spackman, *CRYSTAL EXPLORER® version 3.0, CrystalExplorer 3.0*, University of Western Australia, Perth, Australia, http://hirshfeldsurface.net, 2009.
40 A. D. Bond, *New J. Chem.*, 2004, **28**, 104–114.
41 A. van Langevelde, R. Peschar and H. Schenk, *Chem. Mater.*, 2001, **13**, 1089–1094.

42 V. R. Thalladi, M. Nusse and R. Boese, *J. Am. Chem. Soc.*, 2000, **122**, 9227–9236.
43 V. R. Thalladi, R. Boese and H.-C. Weiss, *Angew. Chem., Int. Ed.*, 2000, **39**, 918–922.
44 S. S. Kuduva, J. A. R. P. Sarma, A. K. Katz, H. L. Carrell and G. R. Desiraju, *J. Phys. Org. Chem.*, 2000, **13**, 719–728.
45 A. Gavezzotti, *J. Chem. Soc., Perkin Trans. 2*, 1995, **2**, 1399–1404.
46 F. E. Karasz and J. A. Pople, *J. Phys. Chem. Solids*, 1961, **20**, 294–306.
47 J. A. Pople and F. E. Karasz, *J. Phys. Chem. Solids*, 1961, **18**, 28–39.
48 F. Di Salvo, B. Camargo, Y. García, F. Teixidor, C. Viñas, J. Giner Planas, M. E. Light and M. B. Hursthouse, *CrystEngComm*, 2011, **12**, 5788.
49 S. Grabowsky, P. M. Dean, B. W. Skelton, A. N. Sobolev, M. A. Spackman and A. H. White, *CrystEngComm*, 2012, **14**, 1083.
50 J. Calvo-Castro, M. Warzecha, A. R. Kennedy, C. J. McHugh and A. J. McLean, *Cryst. Growth Des.*, 2014, **14**, 4849–4858.
51 B. P. Dimitrijević, S. Z. Borozan and S. Đ. Stojanović, *RSC Adv.*, 2012, **2**, 12963–12972.
52 D. Tripathy, V. Ramkumar and D. K. Chand, *Cryst. Growth Des.*, 2013, **13**, 3763–3772.
53 C. P. Frizzo, M. A. P. Martins, M. R. B. Marzari, P. T. Campos, R. M. Claramunt, M. A. García, D. Sanz, I. Alkorta and J. Elguero, *J. Heterocycl. Chem.*, 2010, **47**, 1259–1268.
54 C. P. Frizzo, E. Scapin, P. T. Campos, D. N. Moreira and M. A. P. Martins, *J. Mol. Struct.*, 2009, **933**, 142–147.
55 *Bruker, APEX2 (Version 2.1), COSMO (Version 1.56), BIS (Version 2.0.1.9) SAINT (Version 7.3A) and SADABS (Version 2004/1) and XPREP (Version 2005/4)*, Bruker AXS Inc., Madison, Wisconsin, USA, 2006.
56 G. M. Sheldrick, *Acta Crystallogr., Sect. A: Found. Crystallogr.*, 2008, **64**, 112–122.
57 P. Coppens, L. Leiserowitz and D. Rabinovich, *Acta Crystallogr.*, 1965, **18**, 1035–1038.
58 M. J. Frisch, G. W. Trucks, H. B. Schlegel, G. E. Scuseria, M. A. Robb, J. R. Cheeseman, G. Scalmani, V. Barone, B. Mennucci, G. A. Petersson, H. Nakatsuji, M. Caricato, X. Li, H. P. Hratchian, A. F. Izmaylov, J. Bloino, G. Zheng, J. L. Sonnenberg, M. Hada, M. Ehara, K. Toyota, R. Fukuda, J. Hasegawa, M. Ishida, T. Nakajima, Y. Honda, O. Kitao, H. Nakai, T. Vreven, J. A. Montgomery Jr, J. E. Peralta, F. Ogliaro, M. Bearpark, J. J. Heyd, E. Brothers, K. N. Kudin, V. N. Staroverov, R. Kobayashi, J. Normand, K. Raghavachari, A. Rendell, J. C. Burant, S. S. Iyengar, J. Tomasi, M. Cossi, N. Rega, J. M. Millam, M. Klene, J. E. Knox, J. B. Cross, V. Bakken, C. Adamo, J. Jaramillo, R. Gomperts, R. E. Stratmann, O. Yazyev, A. J. Austin, R. Cammi, C. Pomelli, J. W. Ochterski, R. L. Martin, K. Morokuma, V. G. Zakrzewski, G. A. Voth, P. Salvador, J. J. Dannenberg, S. Dapprich, A. D. Daniels, O. Farkas, J. B. Foresman, J. V. Ortiz, J. Cioslowski and D. J. Fox, *Gaussian® version 09, Revision A.1*, Gaussian, Inc., Wallingford CT, 2009.
59 S. F. Boys and F. Bernardi, *Mol. Phys.*, 1970, **19**, 553–566.

Thermodynamic, Energetic, and Topological Properties of Crystal Packing of Pyrazolo[1,5-a] Pyrimidines Governed by Weak Electrostatic Intermolecular Interactions

Citation:

Frizzo, Clarissa P., Aniele Z. Tier, Izabelle M. Gindri, Alexandre R. Meyer, et al. 2015. "Thermodynamic, energetic, and topological properties of crystal packing of pyrazolo[1,5-a] pyrimidines governed by weak electrostatic intermolecular interactions." CrystEngComm 17(23), doi: 10.1039/c5ce00613a